

Exploring the validity of $Z = 38$ and $Z = 50$ proton closed shells in even-even Mo isotopes

H. Dejbakhsh, D. Latypov, G. Ajupova, and S. Shlomo
Cyclotron Institute, Texas A&M University, College Station, Texas 77843
 (Received 24 June 1992)

Energy spectra, $B(E2)$ values, and ratios of the neutron-rich even-even Mo isotopes in the mass 100 region have been investigated in terms of the neutron-proton interacting boson model. Two different approaches were used. The first investigation is based on the validity of the $Z = 38$ subshell closure considering ^{88}Sr as a doubly magic core. In the second calculation $Z = 50$ and $N = 50$ were considered as valid closed shells leading to ^{100}Sn as a core. The results from both calculations are compared with experimental data.

PACS number(s): 21.60.Fw, 23.20.Lv, 23.20.-g, 27.60.+j

I. INTRODUCTION

The first excited 0^+ levels in the Mo isotopes are low in energy, have a minimum in ^{98}Mo , and are near or below the first 2^+ energies. This has been associated with shape coexistence in these nuclei. The origin of the strong deformation and coexistence of two shapes in this region can be attributed to the existence of the $Z = 38, 40$ and $N = 56$ subshells and neutron-proton interaction. It was shown [1] that the deformed state can coexist with a nearly spherical configuration in a delicate balance. In this region, which shape is lower depends on the number of neutrons. It is a challenge to the theoretical model to give a good description of the transitional nuclei, which lie between spherical and deformed regions, such as $^{94-100}\text{Mo}$.

Sambataro and Molnar [1] have investigated the low-lying structure of the Mo isotopes within the framework of the interacting boson (IBM-2) model including the mixing of two boson configurations [2]. This calculation exhibited a good agreement with the known properties of these nuclei. The first configuration consists of one proton boson and two to six neutron bosons ($A = 96-104$) assuming the closed shells of $Z = 40$ and $N = 50$. The second configuration corresponds to the excited pair of proton bosons out of the $Z = 40$ shell resulting in three proton bosons, two proton bosons, and one proton hole boson. The first configuration provides the dominant contribution to the ground-state wave function of the lighter Mo isotopes. The second configuration is the dominant configuration for the heavier Mo isotopes. This investigation indicates a spherical shape for the ground state in lighter Mo isotopes ($^{96-98}\text{Mo}$), and a deformed shape for the heavier Mo isotopes ($^{102-104}\text{Mo}$), see parameters in Table I of Ref. [1]. In Ref. [1] the values of χ_π and χ_ν were chosen the same as those in the Ru isotopes. Since these parameters reflect the direction of the shape transition, we expect the values of these parameters to be different from those in the Ru isotopes. The shape transition in the Ru isotopes is from a vibrational [U(5)] limit in the lighter isotopes to a γ -unstable [O(6)] limit in the heavier isotopes [3]. But, the shape transition in the Mo isotopes is known [4] to be from a vibrational limit in

$^{94-96}\text{Mo}$ to a rotational limit in $^{102-104}\text{Mo}$.

The Mo isotopes have been investigated in the framework of IBM-1 assuming an effective boson number derived from either configuration mixing or an $N_n N_p$ scheme [5]. The parameter χ , which is related to quadrupole strength, has a large negative value, $\chi = -1.12$, in contrast to that of mixing calculations [$\chi = (\chi_\pi + \chi_\nu)/2 = -0.3$]. The overall agreement with data is reasonable, but a large discrepancy exists between the theoretical values and some of the experimental $B(E2)$ values in the case of the effective boson calculation. This is an indication of a limitation of the effective boson approach.

The microscopic investigation of the Zr and Mo isotopes, carried out by Federman and Pittel [4] in the shell model and Hartree-Fock-Bogoliubov framework, considered $Z = 38$ and $N = 50$ as closed shells for protons and neutrons, respectively. The study showed that the deformation is produced by the isoscalar part of the neutron-proton ($n-p$) interaction in this region. Based on this investigation we considered $Z = 38$ instead of $Z = 40$, which has been chosen in the Sambataro and Molnar study, as a core [1]. As we shall see, our results support the microscopic investigation of Federman and Pittel that the $n-p$ interaction of valence particles outside the core ^{88}Sr nucleus ($Z = 38$ and $N = 50$) is necessary to describe these nuclei.

In this paper we present the results of two different calculations for neutron-rich even-even Mo isotopes without introducing the mixing of two boson configurations. The first calculation considers the $Z = 38$ subshell as a valid shell as it was in the Federman and Pittel calculation. The inert core in this case is ^{88}Sr . The second calculation is based on shell-model considerations of the $Z = 50$ closed shell, in this case the inert core is ^{100}Sn . In this case the assumption that $Z = 38$ is a valid closed shell is not required (one can assume $Z = 28$). We carried out this calculation in order to answer the question on the validity of the $Z = 38$ subshell closure. The specific IBM-2 model is described in Sec. II and the procedure is discussed in Sec. III. The results from both calculations are compared with experimental data in Sec. IV. In Sec. V, the electromagnetic transitions are described and the theoretical and experimental $B(E2)$'s and ratios are com-

pared. The conclusion of this investigation is presented in Sec. VI.

II. THE NEUTRON-PROTON INTERACTING BOSON MODEL

The general form of the IBM-2 Hamiltonian can be written [6]

$$H = H_\nu + H_\pi + H_{\nu,\pi}, \quad (1)$$

which consists of the neutron boson, proton boson, and neutron boson-proton boson interaction Hamiltonians.

The IBM-2 Hamiltonian used in this calculation is written as follows:

$$H_\rho = \varepsilon_\rho n_{d\rho} + V_{\rho\rho}, \quad \rho = \nu, \pi, \quad (2)$$

$$H_{\nu,\pi} = \kappa(Q_\nu \cdot Q_\pi) + M_{\nu,\pi}, \quad (3)$$

where the quadrupole operator, proton-proton, neutron-neutron, and Majorana interactions are written, respectively, as follows:

$$Q_\rho = d_\rho^\dagger s_\rho + s_\rho^\dagger d_\rho + \chi_\rho [d_\rho^\dagger \tilde{d}_\rho]^{(2)}, \quad (4)$$

$$V_{\rho\rho} = \frac{1}{2} \sum_{L=0,2,4} C_\rho^{(L)} ([d_\rho^\dagger d_\rho^\dagger]^{(L)} \cdot [\tilde{d}_\rho \tilde{d}_\rho]^{(L)}), \quad (5)$$

$$M_{\nu,\pi} = \frac{1}{2} \xi_2 (d_\nu^\dagger s_\pi^\dagger - d_\pi^\dagger s_\nu^\dagger) \cdot (\tilde{d}_\nu s_\pi - \tilde{d}_\pi s_\nu) + \sum_{K=1,3} \xi_K ([d_\nu^\dagger d_\pi^\dagger]^{(K)} \cdot [\tilde{d}_\nu \tilde{d}_\pi]^{(K)}). \quad (6)$$

The Majorana term describes the interaction between proton and neutron bosons which acts on the states antisymmetric under the interchange of neutron and proton bosons. $n_{d\rho}$ is the d boson number operator, $s_\rho^\dagger, d_\rho^\dagger$ and s_ρ, d_ρ create and annihilate neutron bosons ($\rho = \nu$) and proton bosons ($\rho = \pi$). The main parameters in these calculations are $\varepsilon_\nu, \varepsilon_\pi$, which determine the energy of the neutron and proton d bosons relative to the s bosons, respectively, κ the quadrupole-quadrupole interaction strength, χ_ν and χ_π are the quadrupole structure parameters of the neutron and proton bosons, respectively; and the Majorana parameters ξ_1, ξ_2 , and ξ_3 . For more details on this model see Ref. [6].

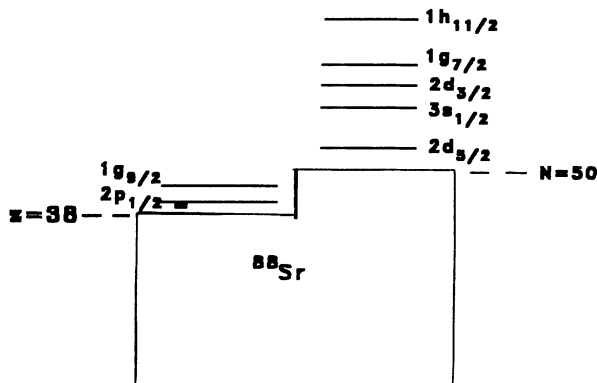


FIG. 1. Single-particle levels in the mass 100 region, assuming an ^{88}Sr core.

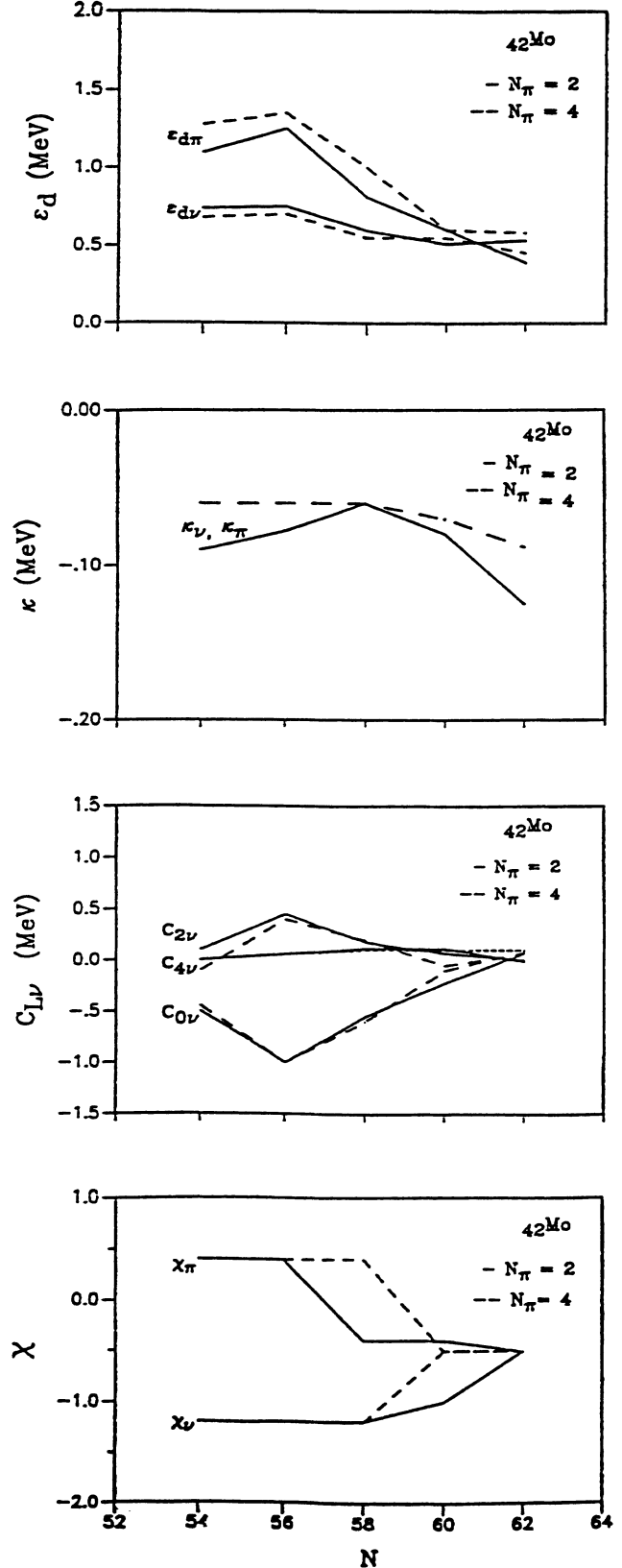


FIG. 2. Determined values for the parameters $\varepsilon_\nu, \varepsilon_\pi, \kappa, \chi_\nu, \chi_\pi$, and $c_{L\nu}$ for even-even Mo isotopes in the mass 100 region. The solid lines are parameters for $N_\pi = 2$ and the dashed lines are for $N_\pi = 4$ calculations.

III. PROCEDURE

We have performed two separate IBM-2 calculations using the Hamiltonian of Eq. (2). The first calculation is based on the validity of the $Z=38$ subshell closure. Figure 1 shows the relevant single-particle levels from the shell-model point of view appropriate for the ^{88}Sr inert core. In this case the interacting boson model calculation for Mo isotopes considers $N_\pi=2$ (two active pairs of protons above $Z=38$, see Fig. 1), and $N_\nu=2-6$ for $^{96-104}\text{Mo}$ isotopes.

In principal all parameters can be varied independently in order to fit the energy and the electromagnetic properties of one nucleus. However, in order to reduce the number of free parameters we only allowed ϵ_ν , ϵ_π , κ , χ_ν , χ_π , and $c_{1\nu}$ to vary as a function of N_ν . Figure 2 shows all the parameters used in this calculation ($N_\pi=2$) as solid lines.

In order to investigate further the validity of the $Z=38$ subshell closure in comparison with the $Z=50$ closed shell, we carried out the second investigation of the IBM-2 model for Mo isotopes considering the $Z=50$ and $N=50$ closed shells. Here, the interacting boson model assumes $N_\pi=4$ (four pairs of proton-hole bosons from the $Z=50$ shell) with the same number of neutron bosons as in the first calculation. As it was pointed out earlier, in this case we do not assume that $Z=38$ is a valid closed shell. The parameters for the IBM-2 calculation with $N_\pi=4$ are shown in Fig. 2 as dashed lines. The parameters have similar behavior to those for $N_\pi=2$. ϵ_π is larger for the four proton-hole bosons than the two proton boson calculations.

In Ref. [1] the relative energy of the neutron d bosons to the neutron s bosons, ϵ_ν , was chosen equal to the proton boson, for each configuration. As far as we know, to date, all other IBM-2 calculations also assumed $\epsilon_\nu = \epsilon_\nu = \epsilon_\pi$. When neutrons and protons are added to the ^{88}Sr

core they do not fill the same orbitals. As seen from Fig. 3, the data show that the excitation energy of the first 2^+ for the nuclei obtained by adding a pair of protons to the ^{88}Sr core is significantly larger than that of the 2^+ of the nuclei obtained by adding a pair of neutrons to the ^{88}Sr core. Therefore, in our calculations we have taken $\epsilon_\nu \neq \epsilon_\pi$. The interaction between the protons in the $1g_{9/2}$ orbit and the neutrons in $1g_{7/2}$ is an important deformation driving force in the Mo isotopes and will increase as number of neutrons increases. This has been reflected through the values of ϵ_ν and ϵ_π which decreases as the number of neutron increases (see Fig. 2). Detailed investigation of the effect of the ϵ_ν value differing from that of ϵ_π will be discussed in next section.

The additional difference between our calculation and the previous study are the values of χ_ν and χ_π . In Ref. [1] the authors have chosen neutron quadrupole strength, χ_ν , and proton quadrupole strength, χ_π , for the Mo isotopes the same as those in the Ru isotopes. For $^{96-98}\text{Mo}$ the same value of χ_ν and χ_π predicts the best $B(E2)$ values and ratios. For $^{100-104}\text{Mo}$ the different values of χ_ν and χ_π resulted in better agreement for $B(E2)$ values and ratios. Figure 2 shows these parameter which vary smoothly as a function of the neutron boson number. The values of χ_ν and χ_π have the same sign for the $^{100-104}\text{Mo}$ isotopes and in ^{104}Mo the amplitudes are also the same. The value of χ_ν and χ_π for $^{100-104}\text{Mo}$ and their amplitudes are an indication that the shape transition is toward the SU(3) limit.

The effect of the proton-proton boson interaction, $V_{\pi\pi}$, for the Mo isotopes was negligible, therefore it was ignored in both calculations. The Majorana parameter separates the states with mixed proton-neutron symmetry with respect to the totally symmetric one. The effect of the Majorana's force on the low-lying energy spectra was small and it was kept constant throughout both calculations.

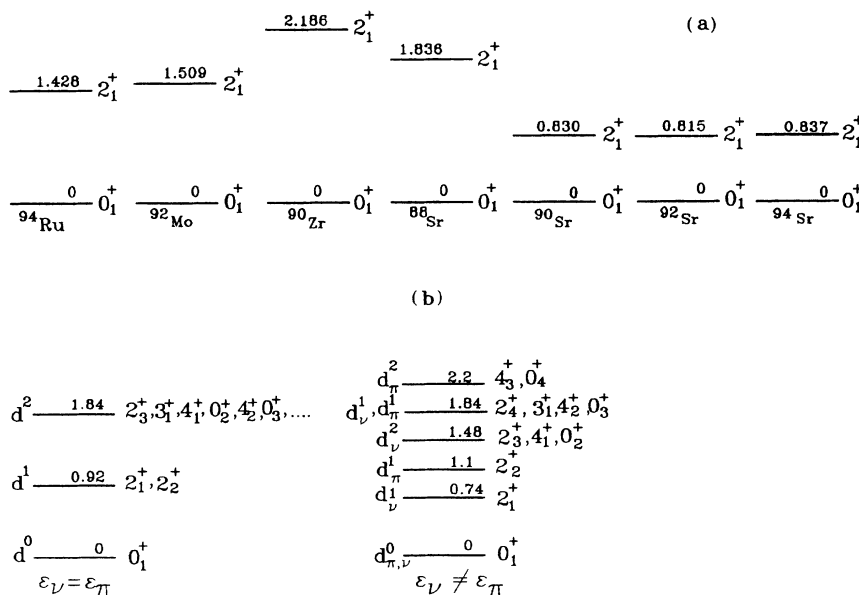


FIG. 3. (a) Experimental excitation energy of the first 2^+ states for some of the nuclei in the mass 100 region, taken from Ref. [10]. (b) The schematic spectra for a nucleus with one neutron and one proton bosons. The spectrum for $\epsilon_\nu = \epsilon_\pi = 0.92$ MeV is shown on the left side and $\epsilon_\nu \neq \epsilon_\pi$ ($\epsilon_\nu = 0.74$ and $\epsilon_\pi = 1.1$ MeV) on the right side.

IV. THE ENERGY SPECTRA

Figure 3 shows the first excited 2^+ state of ^{88}Sr (core nucleus for Mo isotopes), ^{90}Sr , and ^{90}Zr . The $E(2_1^+)$ value for ^{90}Sr corresponds to the excitation energy of the neutron d boson ($N_\nu=1$) from ^{88}Sr and $E(2_1^+)$ of ^{90}Zr corresponds to the excitation energy of the proton d boson ($N_\pi=1$). The energy of the first 2^+ state in ^{90}Zr is high relative to the energy of the first 2^+ state of the nuclei with four or six protons added (^{92}Mo , ^{94}Ru , see Fig. 3) to the ^{88}Sr core. Therefore, an effective excitation energy was considered for the proton d boson. The energy of the first excited states of the nuclei are similar when two, four, or six neutrons are added to the ^{88}Sr core. In our calculations the values of ϵ_ν and ϵ_π are close to the value of $E(2_1^+)$ for ^{90}Sr and ^{92}Mo , respectively. In order to investigate the effect of ϵ_ν differing from ϵ_π we performed two calculations in the $U(5)$ limit. Figure 3 shows the result of the IBM-2 calculation for $N_\pi=1$ and $N_\nu=1$. In the first calculation $\epsilon_\nu=\epsilon_\pi=0.92$ MeV and in the second calculation ϵ_ν is not equal to ϵ_π ($\epsilon_\nu=0.74$ MeV and $\epsilon_\pi=1.1$ MeV), all the other IBM-2 parameters are zero. This figure shows how some of the degeneracy is removed by taking the ϵ_ν value different from that of ϵ_π . This also explains why we are successful in reproducing the correct excitation energy levels of the Mo isotopes without introducing the mixing of two configurations.

In our calculation the energy spectra are very sensitive to the energy of the proton and neutron d bosons. The ϵ_π in our calculation has a similar value to ϵ of the first configuration, $N_\pi=1$ in the IBM-2 mixing calculation [1], for Mo isotopes with $N < 60$, and ϵ_ν has a value similar to that of the second configuration, $N_\pi=3$. Typically ϵ decreases from the beginning of the shell up to the middle of the shell and increases as it moves toward the end of the shell. Most of the parameters vary smoothly (see Fig. 2), with the only unusual behavior of ϵ being for the nucleus with a neutron number equal to 56. The value of ϵ decreases as the neutron number increases, but as it can be seen from Fig. 2 the value of ϵ increases as a pair of neutrons is added (54 to 56). This is related to the presence of the $N=56$ subshell closure. The collectivity of this nucleus relative to the neighboring nucleus ($N=54$), $E_{4_1^+}/E_{2_1^+}$ of 2.09 for ^{96}Mo compared to the 1.92 value for ^{98}Mo , reflects a similar behavior. The other important fact is the values of ϵ_π and ϵ_ν for $N > 60$. In our work the value of ϵ_ν became close to that of ϵ_π ; this is due to the fact that the $1g_{7/2}$ orbital is being filled. The parameter κ behaves the same as those of Ref. [1] but the values are larger in our calculation.

In this investigation we paid special attention to the second 0^+ and second 2^+ in addition to the first 3^+ state because these states have been associated with shape coexistence [7]. The excitation energies for all of the low-lying levels could be reproduced very well due to different values of ϵ for neutron and proton bosons. In Fig. 4, we have plotted the excitation energies of the even yrast levels for $J^\pi=2^+-6^+$ for Mo isotopes, $A=96-104$. The solid lines are calculated excitation energies for $N_\pi=2$. The experimental energies are given by points

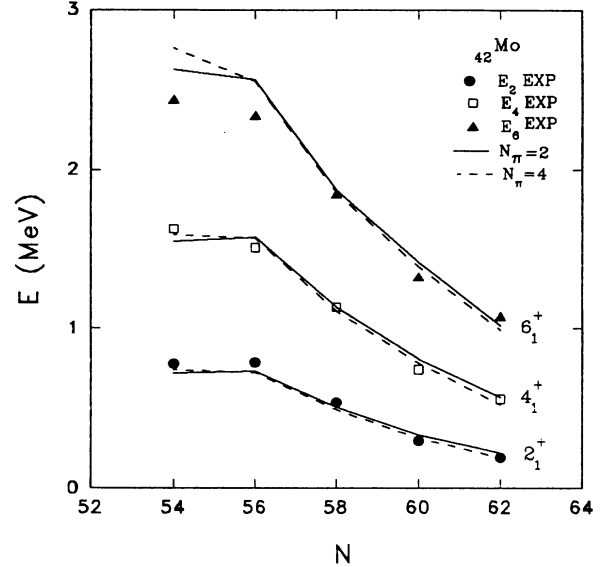


FIG. 4. Excitation energy of the yrast levels with angular momentum J and parity π , (J^π) for Mo isotopes. The data are taken from Refs. [11–15].

representing different angular momenta as shown in the figure. The excitation of higher angular momentum states is more interesting. We have observed a deviation between theory and experimental values of $J^\pi=8^+$ and 10^+ , especially for ^{96}Mo with fewer neutron bosons. However, one must be careful comparing higher spin states because alignment occurs, for neutron-rich nuclei in the mass 100 region, at spin $12\hbar$ [8]. In order to compare the results with higher angular momentum states one has to consider the excitation of a pair of neutrons; see the approach of Ref. [9].

In Figure 5, the result of the calculation for the

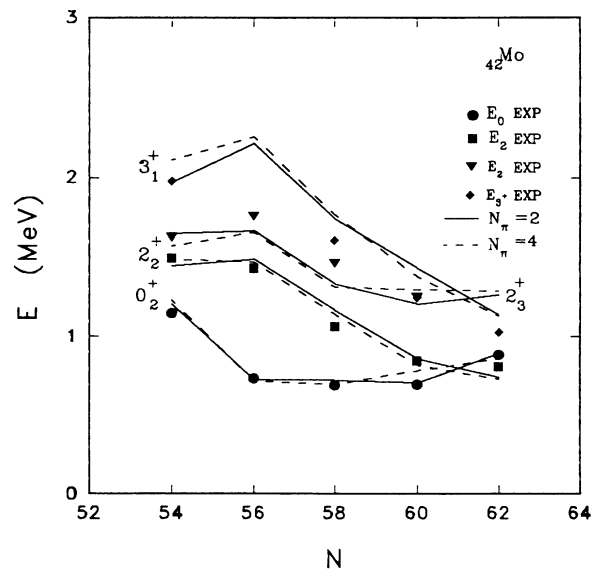


FIG. 5. Excitation energy of the i th levels with angular momentum J and parity π , (J^π) for Mo isotopes. Data points are taken from Refs. [11–15].

$J^\pi=0_2^+, 2_2^+, 2_3^+$, and 3_1^+ states is compared with the experimental data for Mo isotopes, $A=96-104$. The solid lines in Fig. 5 show the results of the $N_\pi=2$ calculation for 0_2^+ that has been associated [1] with the second shape along with $2_2^+, 2_3^+$, and 3_1^+ . The agreement of the result from IBM-2 with $N_\pi=2$ with the experimental result is good (see Fig. 5). Most of the features related to the shape coexistence described by the mixing calculation [1] can be described by this calculation equally well. This result shows that when considering $Z=38$ as a proton closed shell the IBM-2 can properly predict the property of the Mo isotopes.

The result from the investigation with $N_\pi=4$ for the yrast band of Mo isotopes is also shown in Fig. 4 and the other states are shown in Fig. 5 as dashed lines. As shown in the figures, the results from both calculations are almost the same and in good agreement with experimental data.

V. ELECTROMAGNETIC TRANSITIONS

The electromagnetic properties of the Mo isotopes have been calculated using the following boson $E2$ operator:

$$T(E2) = e_\nu Q_\nu + e_\pi Q_\pi, \quad (7)$$

where the quadrupole operators, $Q_{\nu(\pi)}$, are defined in Eq. (3). In principle the values of e_ν and e_π could be different from each other and each nucleus. But we have chosen one value, $e_B = e_\nu = e_\pi = 0.106 e b$, fixed for both calculations. The calculated and experimental $B(E2; 2_1^+ \rightarrow 0_1^+)$ values are shown in Fig. 6 with symbols representing the data. The solid lines are the calculated values for the $N_\pi=2$ case and the dashed lines are the calculated result from $N_\pi=4$. In the $N_\pi=2$ calculation we did not predict

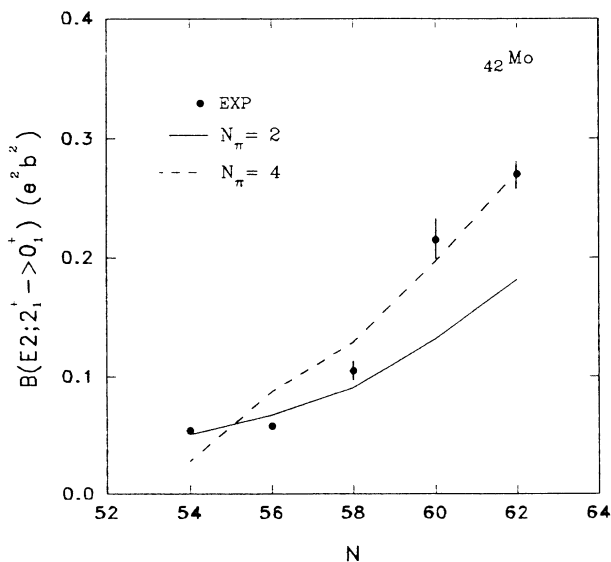


FIG. 6. $B(E2; 2_1^+ \rightarrow 0_1^+)$ values for the Mo isotopes. The data are taken from Refs. [11–15]. The solid line is a result of the calculation with $N_\pi=2$ and the dashed line is with $N_\pi=4$. Experimental data are shown as symbols.

as steep an increase for $B(E2; 2_1^+ \rightarrow 0_1^+)$ as seen in the experimental data when going from $N=58$ to 62 , but the $N_\pi=4$ calculation predicts this trend very well (see Fig. 6). The energy level spectrum is not very sensitive to the χ values but the electromagnetic transitions are. Considering a small positive value for χ_π (0.4) for ^{96}Mo we have improved the $B(E2)$ values, especially the $B(E2; 2_2^+ \rightarrow 2_1^+)/B(E2; 2_1^+ \rightarrow 0_1^+)$ and $B(E2; 2_3^+ \rightarrow 2_1^+)/B(E2; 2_1^+ \rightarrow 0_1^+)$ ratios. This was not true for heavier nuclei in the chain.

In order to explore further the nature of the shape transition, the experimental $B(E2; 2_1^+ \rightarrow 0_1^+)$ values were compared with the results from three limiting cases [U(5), SU(3), and O(6)]. Figure 7(a) shows the $B(E2)$ for 2_1^+ to

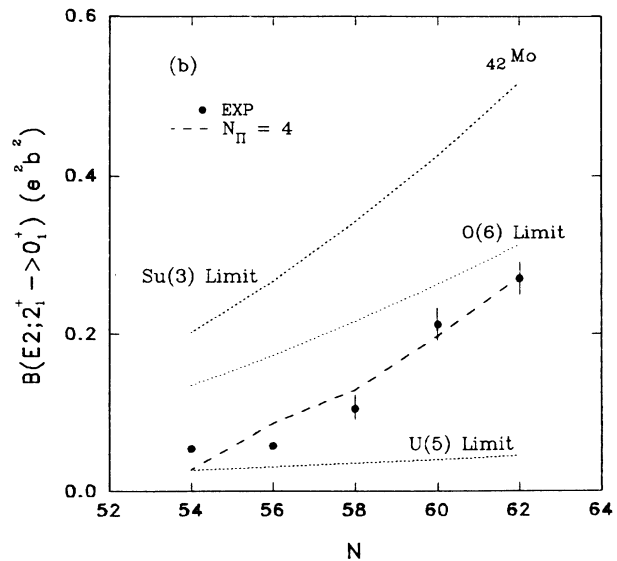
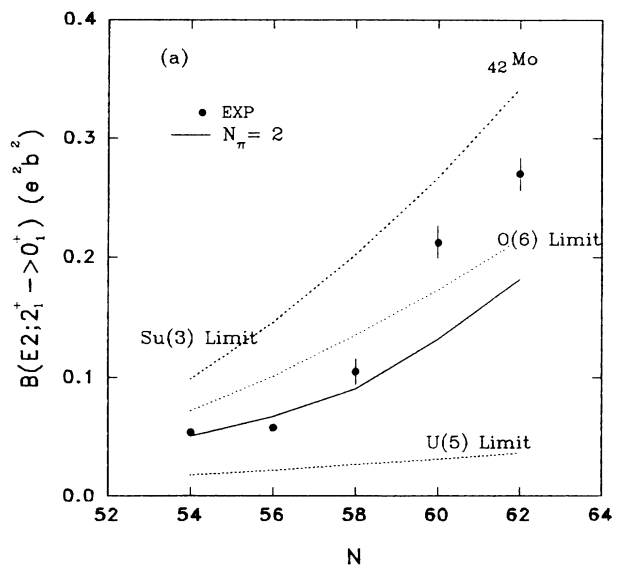


FIG. 7. (a) $B(E2; 2_1^+ \rightarrow 0_1^+)$ values for the Mo isotopes, with $N_\pi=2$ along with the result for the three limiting cases (see text for detail). The data are taken from Refs. [11–15]. (b) The same as (a) for the $N_\pi=4$ calculation.

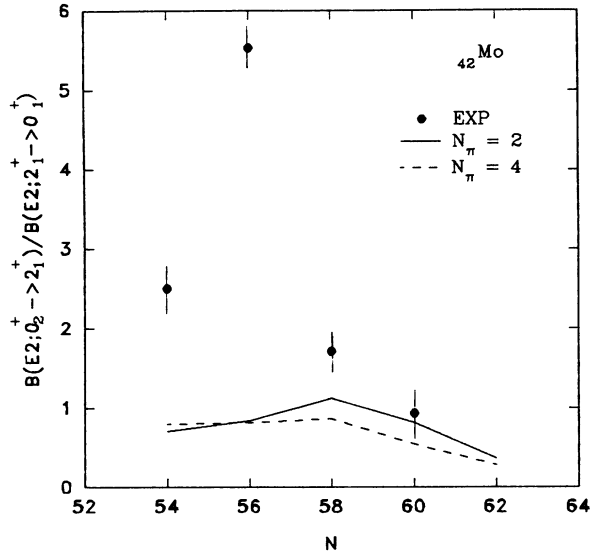


FIG. 8. Experimental (symbols) and calculated values of the $B(E2; 0_2^+ \rightarrow 2_1^+) / B(E2; 2_1^+ \rightarrow 0_1^+)$ ratios. The solid and dashed lines correspond to the $N_\pi=2$ and $N_\pi=4$ calculations, respectively.

0_1^+ transitions for three limiting cases, U(5), SU(3), and O(6), in the IBM-2 as a dotted line along with the result from the $N_\pi=2$ calculation. In Fig. 7(b) we show the same result as Fig. 7(a) but for the $N_\pi=4$ calculation. The calculations for the limiting cases are based on the relations given in Ref. [6] assuming $e_\pi=e_\nu=0.106 e b$. It appears from Fig. 7(b) that the shape transition for the Mo isotopes is from a vibrational toward a γ -unstable [O(6)] limit when these nuclei are treated as four proton-hole bosons. But, Fig. 7(a) shows that the transition for Mo isotopes is toward the rotor limit [SU(3)], which is in

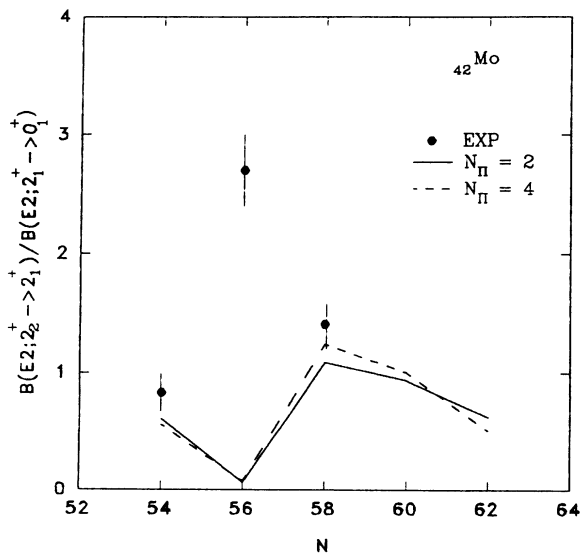


FIG. 9. The same as Fig. 8, for the $B(E2; 2_2^+ \rightarrow 2_1^+) / B(E2; 2_1^+ \rightarrow 0_1^+)$ ratios.

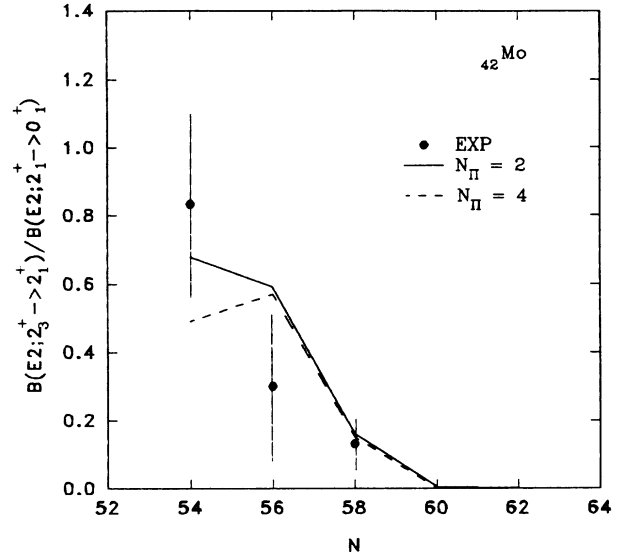


FIG. 10. The same as Fig. 8, for the $B(E2; 2_3^+ \rightarrow 2_1^+) / B(E2; 2_1^+ \rightarrow 0_1^+)$ ratios.

accord with the conclusion of Ref. [4].

The largest discrepancy is found in the $B(E2; 0_2^+ \rightarrow 2_1^+) / B(E2; 2_1^+ \rightarrow 0_1^+)$ ratio which has a sharp increase for $N=56$. In our calculation we did not reproduce this feature. In Ref. [1] it was shown that the 0_2^+ level has a large component from the four-particle-two-hole configuration in the lighter isotopes ($^{96-98}\text{Mo}$). The prediction of the $B(E2; 0_2^+ \rightarrow 2_1^+) / B(E2; 2_1^+ \rightarrow 0_1^+)$ ratio for heavier Mo isotopes ($A=100-104$) is in good agreement with experimental data for both ($N_\pi=2$ and $N_\pi=4$) calculations. The predicted $B(E2; 2_2^+ \rightarrow 2_1^+) / B(E2; 2_1^+ \rightarrow 0_1^+)$ ratio is in good agreement with the experimental data except for ^{98}Mo . The predicted $B(E2; 2_3^+ \rightarrow 2_1^+) /$

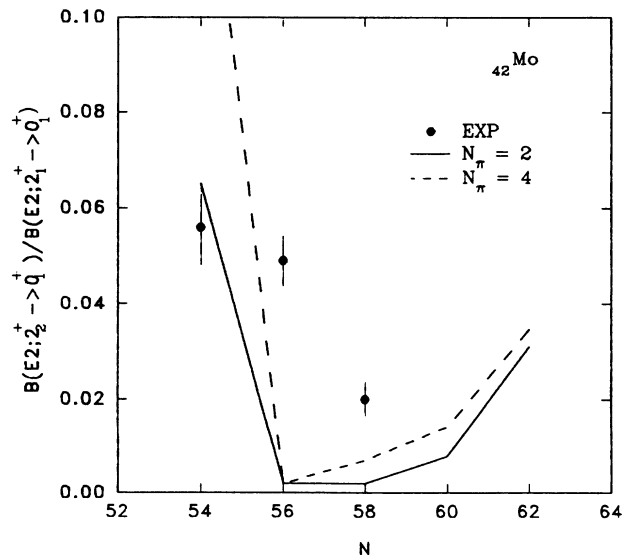


FIG. 11. The same as Fig. 8, for the $B(E2; 2_2^+ \rightarrow 0_1^+) / B(E2; 2_1^+ \rightarrow 0_1^+)$ ratios.

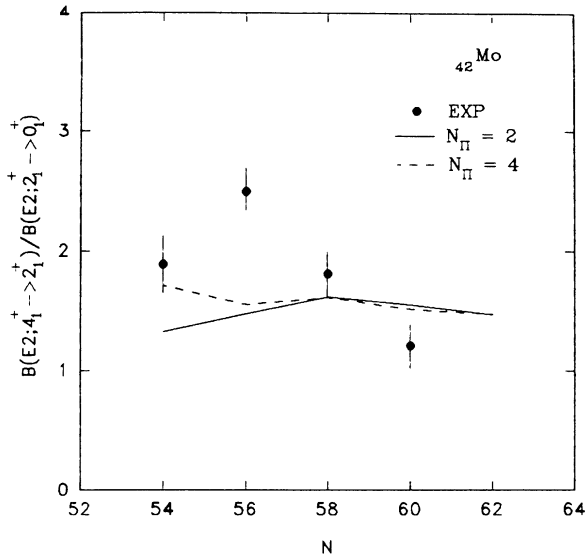


FIG. 12. The same as Fig. 8, for the $B(E2; 4_1^+ \rightarrow 2_1^+)/B(E2; 2_1^+ \rightarrow 0_1^+)$ ratios.

$B(E2; 2_1^+ \rightarrow 0_1^+)$ ratio is in good agreement with the experimental data. The $B(E2; 2_2^+ \rightarrow 0_1^+)/B(E2; 2_1^+ \rightarrow 0_1^+)$ ratio for ^{98}Mo is underestimated in our calculation and in the mixing calculation, but the mixing calculation reproduces the trend. The result of the $B(E2)$ ratios for the $N_\pi=4$ calculation is similar to those of $N_\pi=2$ which are plotted in the same figure (Figs. 6–12) as dashed lines. The overall agreement with the data is reasonable for the Mo isotopes except for ^{98}Mo .

VI. CONCLUSION

In conclusion, the systematic investigation of even-even Mo isotopes in the framework of the IBM-2 has been carried out for two proton bosons and four proton-hole boson configurations. Two sets of calculations were carried out and the results were compared with the experimental data. The calculated results are in good

agreement with the experimental data. We have shown that the low-lying structure of these nuclei can be reproduced equally well by the IBM-2 with two proton bosons or four proton-hole bosons. We add that the parameters of the boson Hamiltonian and the resulting properties of the Mo isotopes for the $N_\pi=4$ case are very similar to those of the $N_\pi=2$ case. This indicates that the $Z=38$ subshell is as valid as the $Z=50$ closed shell. All the features of the nuclei with $N > 58$ can be predicted equally well with both $N_\pi=2$ and $N_\pi=4$ boson configurations.

We have also shown that the low-lying structure of the Mo isotopes can be predicted by the IBM-2 model without introducing the mixing of two configurations by considering the relative energy of the d proton boson to be different from that of the neutron bosons. In this region, where the $n-p$ interaction plays an important role in the deformation driving force, one should consider $\epsilon_v \neq \epsilon_\pi$ which will remove some of the degeneracies.

The calculated $B(E2)$ values for both calculations for the Mo isotopes are in good agreement with the experimental data except for some of the $B(E2)$ ratios of ^{98}Mo . This is due to the first excited 0^+ state which should be considered as an intruder state, similar to the case of the Xe and Pd isotopes [16]. This has confirmed that in some cases that nucleus is very soft, the shape coexistence cannot be ignored in these nuclei.

In summary, we have presented an alternative description for the even-even Mo isotopes in the mass 100 region. We have presented results and shown that $Z=38$ is a valid closed shell as $Z=50$ is for the nuclei in this mass region. We also concluded that the shape transition for these isotopes is from the U(5) limit toward the SU(3) limit.

ACKNOWLEDGMENTS

We wish to thank Prof. T. Otsuka and Prof. N. Yoshida for making their neutron-proton interacting boson code available to us. We acknowledge useful discussions with Prof. B. Barrett and Prof. R. F. Casten. This work was supported in part by NSF Grant Nos. PHY-9110686 and PHY9017008.

- [1] M. Sambataro and G. Molnar, Nucl. Phys. **A376**, 201 (1982).
- [2] P. D. Duval and B. R. Barrett, Nucl. Phys. **A376**, 213 (1982).
- [3] J. Stachel, P. Van Isacker, and K. Heyed, Phys. Rev. C **25**, 650 (1982); P. Van Isacker and G. Puddu, Nucl. Phys. **A348**, 125 (1980).
- [4] P. Federman and S. Pittel, Phys. Rev. C **20**, 820 (1979); P. Federman, S. Pittel, and R. Campos, Phys. Lett. **82B**, 9 (1979).
- [5] G. Catat, D. Bucurescu, D. Cutiou, M. Ivascu, and N. V. Zamfir, Z. Phys. A **335**, 271 (1990).
- [6] F. Iachello and A. Arima, *The Interacting Boson Model* (Cambridge University Press, Cambridge, 1987).
- [7] A. M. Van Den Berg, R. Bijker, N. Blasi, M. Sambataro, R. H. Siemssen, and W. A. Sterrenburg, Nucl. Phys. **A422**,

- 61 (1984).
- [8] D. R. Haenni, H. Dejbakhsh, R. P. Schmitt, and G. Mouchaty, Phys. Rev. C **33**, 1543 (1986).
- [9] N. Yoshida, A. Arima, and T. Otsuka, Phys. Lett. **114B**, 86 (1982).
- [10] *Table of Isotopes*, 7th ed., edited by C. M. Lederer and V. S. Shirely (Wiley, New York, 1978).
- [11] H. W. Mueller, Nucl. Data Sheets **35**, 281 (1982).
- [12] H. W. Mueller, Nucl. Data Sheets **39**, 467 (1983).
- [13] D. Hook, J. L. Durell, W. Gellety, J. Lukasiak, and W. R. Phillip, J. Phys. G **12**, 1277 (1986).
- [14] P. De Gelder, Nucl. Data Sheets **63**, 373 (1990).
- [15] J. Blachot, Nucl. Data Sheets **64**, 1 (1991).
- [16] P. Van Isacker and G. Puddu, Nucl. Phys. **A348**, 125 (1980); J. M. Arias and C. E. Alonso, *ibid.* **A445**, 333 (1985).